

Case Report

Cogan-Reese syndrome: image analysis with specular microscopy, optical coherence tomography, and ultrasound biomicroscopy

Denise Loya-Garcia, MD, Julio C. Hernandez-Camarena, MD, Jorge E. Valdez-Garcia, MD, PhD, and Alejandro Rodríguez-García, MD

Author affiliations: Tecnológico de Monterrey, School of Medicine and Health Sciences, Institute of Ophthalmology and Visual Sciences, Monterrey, Mexico

Summary

Iridocorneal endothelial (ICE) syndrome is a progressive clinical spectrum of corneal endothelial abnormalities affecting the cornea, iris, and iridocorneal angle. Three clinical variations are recognized: essential (progressive) iris atrophy, Chandler syndrome, and Cogan-Reese syndrome. Direct slit-lamp visualization of the cornea and anterior segment in cases of ICE syndrome is inadequate for precise and objective assessment of the affected structures. We describe the evolution of corneal and anterior segment structural changes in a woman with Cogan-Reese syndrome using three different methods of image analysis: specular microscopy, anterior segment optical coherence tomography, and ultrasound biomicroscopy.

Introduction

Cogan-Reese syndrome is a clinical variation of the iridocorneal endothelial (ICE) syndrome characterized by multiple small pedunculated round nodules on the anterior iris surface, iris atrophy, heterochromia, ectropion uveae, and ectopic pupil, as well as corneal edema and iridocorneal angle abnormalities.^{1–5} Anterior segment slit-lamp visualization becomes limited as the disease progresses due to corneal stromal edema. The use of imaging technologies such as specular microscopy (SM), anterior segment spectral domain optical coherence tomography (SD-OCT), and ultrasound biomicroscopy (UBM) allow an objective analysis of the progression, grade, and staging of the disease. Hence, these imaging technologies can help with surgical planning in advanced cases.⁶

Case Report

A 46-year-old woman presented at the Institute of Ophthalmology and Visual Sciences, Monterrey, Mexico, with a complaint of intense photophobia and blurred vision in the mornings in her right eye. Her medical history was significant for glaucoma in her right eye, treated with a trabeculectomy 5 years previously. At her ini-

tial visit, she was on the following topical regimen: dorzolamide and timolol twice daily, sodium chloride 5% three times daily, prednisolone acetate 1% six times daily, and nepafenac 0.1% twice daily. Corrected distance visual acuity was 20/50 in the right eye and 20/20 in the left eye. Intraocular pressure (IOP) by Goldmann tonometry was 21 mm Hg in the right eye and 15 mm Hg in the left eye. On slit-lamp examination, the right eye showed a flat filtration bleb in the superior quadrant, mild corneal stromal edema, and a beaten-metal appearance in the posterior corneal surface, with central predominance (Figure 1A); multiple pedunculated and pigmented iris nodules surrounded by stromal atrophy areas were observed (Figure 1B–C). Gonioscopy revealed a narrow iridocorneal angle (Shaffer II, inferior and nasal quadrants; Shaffer III, temporal and superior quadrants), with peripheral anterior synechiae of the iris. Fundus examination of the right eye showed an optic nerve with a cup-to-disc ratio of 0.7 and no other alterations. The left eye examination was unremarkable.

Corneal and anterior segment SD-OCT (RTVue-100, Optovue, Fremont, CA) and SM (Specular Microscopy EM-3000, Tomey Corp, Nagoya, Japan) were performed

Published May 31, 2019.

Copyright ©2019. All rights reserved. Reproduction in whole or in part in any form or medium without expressed written permission of the Digital Journal of Ophthalmology is prohibited.

doi:10.5693/djo.02.2019.05.001

Correspondence: Alejandro Rodríguez-García, MD, Instituto de Oftalmología y Ciencias Visuales Centro Medico Zambrano Hellion, Av. Batallón de San Patricio No. 112. Col. Real de San Agustín, Garza García, N.L. CP. 62670 Mexico (email: immuneye@gmail.com).

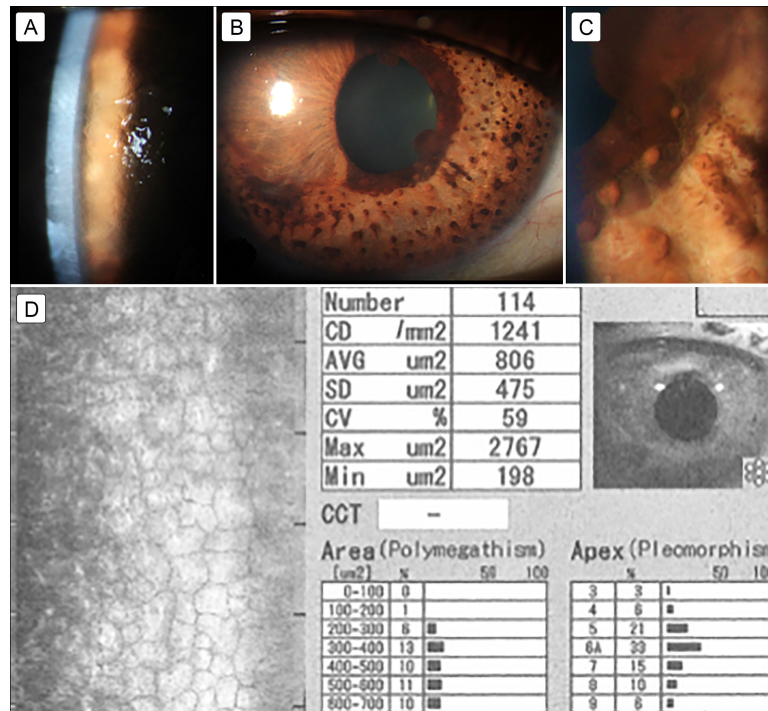


Figure 1. A, Representative slit-lamp photograph showing a “beaten-metal” appearance and moderate stromal edema in the central cornea. B, Prominent nasal ectropion uveae with generalized iris atrophy and multiple pedunculated iris nodules arising in the nasal quadrants. C, Enlarged view showing multiple pigmented iris nodules surrounded by abnormal iris stromal architecture. D, Specular microscopy showing iridocorneal endothelial cells, characterized by a dark area with a central spot of light and a peripheral bright zone as well as a low endothelial cell count, high polymegathism, and pleomorphism.

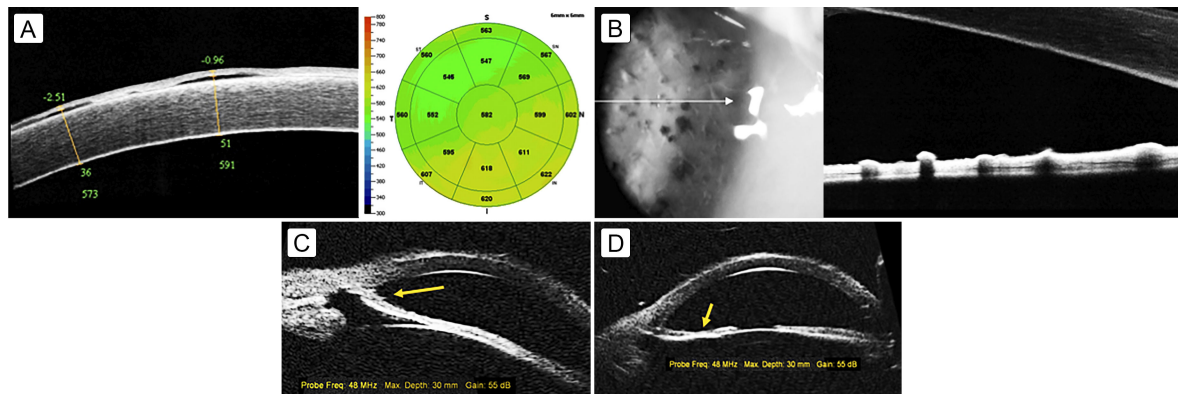


Figure 2. A–B, Spectral domain optical coherence tomography at presentation of the cornea (A), showing subepithelial fluid accumulation with increased central and inferior-nasal corneal thickness, and the anterior segment (B), showing a hyper-reflective membrane, which appears to correspond with abnormal endothelium on the folded anterior iris surface, with multiple rounded Reese nodules. C–D, Ultrasound biomicroscopy images, 2 years after presentation, showing a closed angle with the presence of broad-based, peripheral anterior synechiae (arrow) and a membranelike mound in the iridocorneal angle (C) and an irregular anterior iris surface and marked stromal thinning (arrow) corresponding to iris atrophy (D).

(Figure 2A–B). Areas of subepithelial fluid throughout the cornea and a folded iris surface were observed. The SM showed a low endothelial cell count, polymegath-

ism, and pleomorphism as well as the presence of ICE cells, characterized by a dark area with a central spot of light and a peripheral bright zone (Figure 1D).

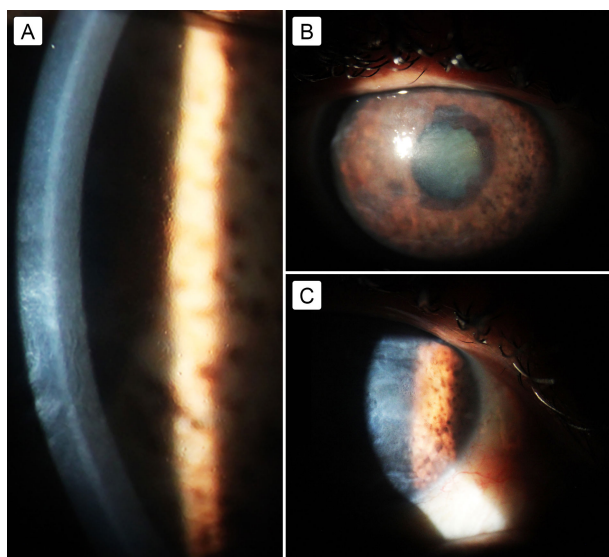


Figure 3. A, Slit-lamp biomicroscopy imaging of the cornea of this patient showing an irregular endothelium and mild stromal edema on presentation. B, The same cornea, 14 months later, with moderate stromal edema that reduces the visibility of iris details. C, Two years after presentation, the cornea shows marked stromal edema, hampering the direct view of the anterior segment.

Topical treatment was modified with the addition of travoprost daily, brinzolamide/timolol twice daily, loteprednol etabonate 0.5% every 6 hours, and sodium chloride 5% twice daily. Follow-up consultations showed a remarkable reduction in the corneal stromal edema; IOP dropped to 12 mm Hg.

Two years later, the patient noticed a significant decrease in vision in the right eye. Slit-lamp examination revealed severe corneal edema, with bullous keratopathy secondary to endothelial dysfunction. Because of significant corneal opacity due to edema, ultrasound biomicroscopy was performed to analyze the disease progression in the anterior segment structures (Figure 2C–D). During this late follow-up period, the cornea became more edematous, and the IOP increased to 27 mm Hg under maximal antiglaucoma therapy (Figure 3A). An Ahmed valve was successfully implanted, lowering the IOP to 16 mm Hg without antiglaucoma eye drops. The patient is awaiting a corneal transplant (Figure 3B–C).

Discussion

In ICE syndrome, the metaplastic endothelial cells begin to migrate posteriorly to Schwalbe's line, blocking the iridocorneal angle, then continue toward the anterior chamber, covering the anterior iris surface and creating an abnormal basal membrane that contracts in several

grades. The contraction leads to ectropion uveae, atrophic damage, and peripheral anterior synechiae of the iris.² On specular microscopy, the ICE cells appear as large, rounded, and pleomorphic cells, showing a specular reflex that clinically corresponds with a “hammered silver bronze” corneal appearance.⁶ Sherrard et al described four morphological patterns: (1) disseminated ICE, characterized by disseminated cells through a healthy endothelium; (2) total ICE, where abnormal cells totally replace the healthy endothelium; (3) subtotal ICE+, characterized by abnormal cells that replace a variable portion of healthy endothelium and the remaining endothelium is composed of small cells; and (4) subtotal ICE–, where abnormal cells replace a variable portion of healthy endothelium which remains composed of enlarged cells.⁷ Our patient was classified in the subtotal ICE– variant, as demonstrated by SM (Figure 2D).

Although these SM morphologic changes are useful for staging the progression of ICE syndrome, endothelial cellular density (ECD) is not a reliable method to measure disease progression because of poor identification of cellular margins, which limits the calculation of the mean cell density. Moreover, the ECD count includes both ICE cells and the remaining healthy endothelial cells; therefore, it may not reflect the true endothelial function.⁸

The iris alterations in this syndrome are distinctive and provide a clue for a definitive diagnosis. Such changes are represented by multiple pedunculated nodules that in early stages of the disease can appear as subtle yellowish nodules that subsequently become more pigmented (Reese nodules) with adjacent iris atrophy, ectropion uveae, and irregular pupil contour.⁹ As can be seen in the current case, the patient presents multiple pedunculated, highly pigmented iris nodules surrounded by stromal iris atrophy, and loss of its crypts. Holló and Naghizadeh used anterior segment SD-OCT to describe the iris characteristics in a patient with Cogan-Reese syndrome.¹⁰ As in their report, we found an irregular iris surface with nummular thickenings corresponding to the pedunculated nodules over the iris surface (Figure 2B). We also noticed hyper-reflectivity on the anterior iris surface, probably corresponding to the abnormal endothelium covering the iris surface, a finding not previously described (Figure 2B); however, we do not have control SD-OCTs or normal irides to state that this is a difference definitively. SD-OCT may also help monitor disease progression. Increased iris folding and thickening, formation of iris nodules, and peripheral anterior synechiae, as well as corneal edema may all be analyzed by serial scans over time.

The progressive course of the disease leads to severe complications, mainly irreversible corneal stromal edema and secondary glaucoma.² See Figure 3. In earlier stages of the disease, gonioscopy is very useful to determine the grade and extent of the anterior chamber angle closure.³ However, once significant endothelial dysfunction occurs, visualization of the angle and the iris is only achieved with the aid of UBM.⁴ Anterior segment UBM is a useful tool for grading the extent of iris atrophy, peripheral anterior synechiae, and proliferative changes in the angle structure.^{4,11} Zhang et al,¹² reporting the results of UBM analysis of 21 patients with ICE syndrome, showed that patients with Cogan-Reese syndrome presented more peripheral anterior synechiae with higher IOP elevation, severe glaucoma, and a greater failure rate of filtering surgery than in the other clinical variants of ICE syndrome. They concluded that UBM is a fast and effective diagnostic method to explore the extent of affected structures in this syndrome and its subtypes and found that UBM analysis has a higher sensitivity than slit-lamp gonioscopy in detecting peripheral anterior synechiae and iris atrophy in patients with advanced Cogan-Reese syndrome. Thus, we recommend conducting a baseline UBM early in this disease to use as a reference, unlike the present case, where SD-OCT was used; although SD-OCT does provide some information, its utility in progressive disease is limited.

The progression of Cogan-Reese clinical manifestations should be evaluated with advanced imaging technologies, which allow a sensitive and objective analysis of the corneal and anterior segment alterations seen in these patients in order to facilitate surgical and therapeutic decision making. To our knowledge, this is the first report of all three imaging modalities being used for anterior segment and corneal analysis for the diagnosis and assessment of a case of Cogan-Reese syndrome.

Literature Search

The authors searched PubMed on January 8, 2018, for English-Language results using the following terms sin-

gly and in combination: *Cogan-Reese syndrome, ICE syndrome, specular microscopy, ultrasound biomicroscopy, and optical coherence tomography.*

References

1. Eagle R, Font R, Yanoff M, Fine B. Proliferative endotheliopathy with iris abnormalities: the iridocorneal endothelial syndrome. *Arch Ophthalmol* 1979;97:2104-11.
2. Shields MB. Progressive essential iris atrophy, Chandler's syndrome, and the iris nevus (Cogan-Reese) syndrome: a spectrum of disease. *Surv Ophthalmol* 1979;24:3-20.
3. Campbell D, Shields M, Smith T. The corneal endothelium and the spectrum of essential iris atrophy. *Am J Ophthalmol* 1978;86:317-24.
4. Scheie H, Yanoff M. Iris Nevus (Cogan-Reese) syndrome: a cause of unilateral glaucoma. *Arch Ophthalmol* 1975;93:963-70.
5. Cogan DG, Reese AB. A syndrome of iris nodules, ectopic Descemet's membrane, and unilateral glaucoma. *Doc Ophthalmol* 1969;26:424-33.
6. Ozdemir Y, Onder F, Coşar CB, Usubütün A, Kural G. Clinical and histopathologic findings of iris nevus (Cogan-Reese) syndrome. *Acta Ophthalmol Scand* 1999;77:234-7.
7. Sherrard, Emil S.; Frangouils, Modea A.; Malcolm, Kerr Muir. On the morphology of cells of posterior cornea in the iridocorneal endothelial syndrome. *Cornea* 1991;10:233-43.
8. Liu YK, Wang IJ, Hu FR, Hung T, Chang HW. Clinical and specular microscopic manifestations of iridocorneal endothelial syndrome. *Jpn J Ophthalmol* 2001;45:281-7.
9. Sacchetti M, Mantelli F, Marengo M, Macchi I, Ambrosio O, Rama P. Diagnosis and management of iridocorneal endothelial syndrome. *Biomed Res Int* 2015;2015:763093.
10. Holló G, Naghizadeh F. Optical coherence tomography characteristics of the iris in Cogan-Reese syndrome. *Eur J Ophthalmol* 2014;24:797-9.
11. Dada T, Gadia R, Sharma A, et al. Ultrasound Biomicroscopy in Glaucoma. *Surv Ophthalmol* 2011;56:433-50.
12. Zhang M, Chen J, Liang L, Laties aM, Liu Z. Ultrasound biomicroscopy of Chinese eyes with iridocorneal endothelial syndrome. *Br J Ophthalmol* 2006;90:64-9.